Received: 2 March 2023 | Revised: 9 April 2024 | Accepted: 10 May 2024

Research Article
Journal of Research and Review in Science
104-116, Volume 11, June 2024
DOI: 10.36108/jrrslasu/4202.11.0180

ORIGINAL RESEARCH

First-Principles Investigations of Band Structure and Thermoelectric Properties of LiYN (Y = Be, Mg, Ca, Sr, and Ba) HalfHeusler Compounds

Bamgbose Muyiwa K.[1], Ayedun Funmilayo.[2], Ogabi C. O.[1], Fabiyi Adegboyega I.[3], Idowu B. A.[1]

[1]Department of Physics, Lagos State University, Ojo. Lagos, Nigeria.

[2]Department of Physics, National Open University of Nigeria

[3]Department of Physics, Federal College of Education Abeokuta.

Correspondence
Bamgbose Muyiwa K., Department of Physics, Faculty of Science, Lagos State University, Nigeria.
Email:muyiwa.bamgbose@lasu.edu.ng

Funding information
This research work is self-sponsored.

Abstract:
Introduction: This work presents a first-principles investigation of the electronic structure and thermoelectric transport coefficients of LiYN(Y = Be, Mg, Ca, Sr, and Ba) half-Heusler(hH) compounds.
Materials and Methods: Density Functional Theory calculation is carried out to investigate the thermoelectric properties of LiYN(Y = Be, Mg, Ca, Sr, and Ba) half-Heusler(hH) compounds.
Aim The work determines the electronic and thermoelectric properties of these compounds.
Results and Discussion: The bandgaps of these compounds range from 2.80eV for LiBeN to 1.01 for LiBaN, and the gap decreases down the group. The band structures of these compounds reveal mixtures of the flat band and parabolic bands. This mixture of bands enhances high-performance thermoelectric behaviours. The thermoelectric transport coefficients calculated in this work are electrical conductivity, thermal conductivity, Seebeck coefficient, power factor, and the dimensionless figure of merit. The figure of merit of LiCaN is 0.99 at the temperature of 1000K; this high figure of merit is due to the perfect flat band and parabolic band in these compounds' conduction band.
Conclusion: From the results obtained in this calculation, these compounds are high-performance thermoelectric candidates.
Keywords: thermoelectric, electronic, half-Heusler, compounds, calculation

All co-authors agreed to have their names listed as authors.

1 INTRODUCTION

The global energy economy needs improvement by renewable energy alternatives to fossil fuel[1]. The choice of colossal dependence on fossil fuel calls for urgent attention from materials scientists. A vast amount of waste heat always accompanies the conversion of fossil fuel to energy. The valuable power obtained from this fuel is greatly reduced by a large portion of the fuel that is converted to waste heat [2]. The conversion of waste heat from fossil fuel combustion needs to be earnest to maximize energy output from fossil fuel. If well addressed, these facts mentioned will reduce the consumption of fossil fuel and thereby reduce the adverse effects of this fuel on the environment and the lives on earth. By minimizing the damaging effects of fossil fuels, the global warming effect will be at the barest minimum.

Thermoelectric generators will convert waste heat to energy. Thermoelectric materials convert waste heat directly to electricity by Seebeck effect[3]-[4]. The thermoelectric materials studied nowadays are compounds and alloys[5]-[11]. The half Heusler compounds are widely studied thermoelectric materials because of their interesting properties like high bulk modulus, high thermal stability, simple crystal structure, high band degeneracy, and tuneable electronic structure[12]-[13]. The half Heusler compounds that are of great importance to the thermoelectric generation of electricity are 8 or 18 electrons Valence Electron Counts(VEC), these 8 or 18 VEC half Heusler compounds are semiconductors, charge carriers of these compounds have high effective mass[14]-[17]. Half of Heusler's compounds belong to space group number 216(F43m) with chemical formula XYZ. The atoms X, Y, and Z are usually at Wycoff's positions (0.50 0.50 0.50), (0.25 0.25 0.25), and (0.00 0.00 0.00), the atomic positions are optimized to know the most stable structure. The conventional Heusler compounds consist of two transition elements X and Y, and main group elements Z, with element Y the heaviest among the three elements occupying position (0.25 0.25 0.25). The VEC 8 half Heusler compounds are topological insulators, thermoelectric and optoelectronic materials. The most studied of 8 VEC half Heusler compounds are I-II-V group compounds[18]-[21] with few reports on their thermoelectric properties.

In the literature, there are few reports on the thermoelectric properties of "Nowotny–Juza" compounds; most of these compounds are promising candidates for optoelectronic industries. Tremendous research works on these compounds centred around electronic and optical properties[22]-[23]. Due to little work on these compounds, the study of hypothetical half-Heusler compounds LiYN(Be, Mg, Ca, Sr, and Ba) will give the necessary data and properties of "Nowotny-Juza" half-Heusler compounds. The electronic band structure, Seebeck coefficient, the figure of merit(ZT), and Electronic Fitness Function(EFF) of these compounds were obtained in this work. Some of the properties calculated in this work are not available in the literature. From the available literature, this work presents the thermoelectric properties of LiBeN, LiMgN, LiCaN, and LiBaN for the first time.

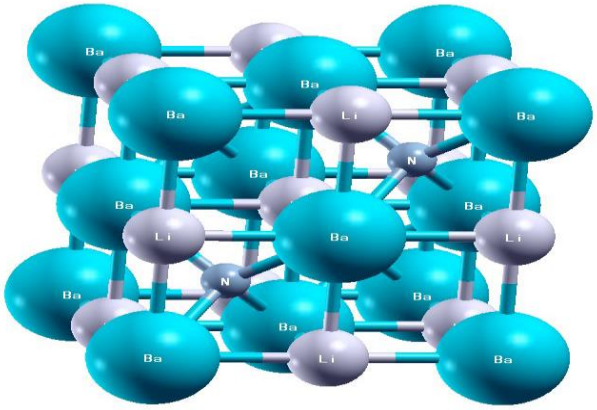

Figure 1: Crystal structure of LiBaN

2 MATERIAL AND METHODS

First-principles Density Functional Theory(DFT) within Generalised Gradient Approximation as implemented in Quantum ESSPRESSO package[25]-[27] was used to calculate structural and electronic properties of LiYN(Be, Mg, Ca, Sr and Ba). Generalized Gradient Approximation (GGA) with Perdew-Burke-Ernzerhof(PBE) parameterization flavour[28] was used to treat exchange-correlation(XC) potential functional. Projector Augmented Wave(PAW) pseudopotential generated by ”atomic” code was used[29] with optimized kinetic energy cut-off of 80Ry to expand plane wave. Brillouin zone (BZ) integration was done by tetrahedron method over a particular set k-points mesh of 12X12X12 using the standard k-point technique of Monkhorst and Pack[30]. Semi-classical Boltzmann theory as implemented in BoltzTrap code[31] with constant relaxation time was used obtained thermoelectric transport coefficients such as Seebeck coefficient, electrical conductivity, electronic thermal conductivity, power factor, and figure of merit, according to the following equations[32];

$$S_{\alpha\beta}(T,\mu) = \frac{1}{eT\Omega\sigma_{\alpha\beta}(T,\mu)} \int \bar{\sigma}_{\alpha\beta}(\varepsilon)(\varepsilon-\mu)\left[\frac{\partial f_o(T,\varepsilon,\mu)}{\partial\varepsilon}\right]d\varepsilon \quad (1)$$

$$\sigma_{\alpha\beta}(T,\mu) = \frac{1}{\Omega}\int \bar{\sigma}_{\alpha\beta}(\varepsilon)\left[-\frac{\partial f_o(T,\varepsilon,\mu)}{\partial\varepsilon}\right]d\varepsilon$$

$$K^o_{\alpha\beta}(T,\mu) = \frac{1}{e^2T\Omega}\int \bar{\sigma}_{\alpha\beta}(\varepsilon)(\varepsilon-\mu)^2\left[-\frac{\partial f_o(T,\varepsilon,\mu)}{\partial\varepsilon}\right]d\varepsilon \quad (3)$$

The transport distribution function $\bar{\sigma}_{\alpha\beta}$ which appears in equations 1-3 is defined as

$$\bar{\sigma}_{\alpha\beta}(\varepsilon) = \frac{e^2}{N}\sum_{i,k}\tau_i V_\alpha(i,\vec{k}).V_\beta(i,\vec{k}).\frac{\delta(\varepsilon-\varepsilon_{i,\vec{k}})}{d\varepsilon} \quad (4)$$

$$PF = S^2\sigma \quad (5)$$

$$zT = (S^2\sigma/k)T \quad (6)$$

where S, σ, k, PF, and zT are the Seebeck coefficient, electrical conductivity, thermal conductivity, power factor, and dimensionless figure of merit. T, μ, Ω, ε, and τ are temperature, chemical potential, volume, band energy, and relaxation time.

3 RESULTS AND DISCUSSION

3.1 Optimised Structure of LiYN(Be, Mg, Ca, Sr and Ba)

The optimized structures of LiYN(Be, Mg, Ca, Sr, and Ba) are obtained by total energy minimization of three phases of these compounds. The phases optimized are as follows; α with Li atom at 4c, Y atom at 4b and N atom at 4a, the β with Li atom at 4b, Y atom at 4a and N atom at 4c, and the γ with Li atom at 4a, Y atom at 4c and N atom at 4b. Table 1 gives The result obtained from the structural optimization of the phases. The most stable phase is the β phase; this is in good agreement with previous results on these compounds. From Table 2, the equilibrium lattice constants obtained in this work for β phase are in excellent agreement with the calculation earlier done on similar Nowotny–Juza phase of half Heusler compounds [32]-[34]. The equilibrium lattice constant of the most stable phase of LiYN(Be, Mg, Ca, Sr, and Ba) increases linearly. The equilibrium lattice constants increase down the group, and this increment varies from 0.34-0.62Å. Reduction in the increment of equilibrium lattice constant is due to the sizeable electrostatic attraction between the electrons and the half Heusler compound's ionic core. The equilibrium lattice constants obtained in this calculation are in excellent agreement with previous theoretical and experimental results shown in Table 2.

3.2 Band Structure

The electronic band structures of LiYN(Y=Be, Mg, Ca, Sr, and Ba) are obtained along high symmetry points $X - W - K - L - \Gamma - X$ in the first Brillouin zone, which is displayed in Figure 2. This work's band structures show all semiconductor band structures with energy bandgap and degenerate bands in the valence band. For LiBeN, the highest occupied band in the valence band, and the lowest unoccupied band in the conduction band occur at Γ high symmetry point in the Brillouin Zone(BZ); therefore, LiBeN has a direct bandgap of 2.80eV. The bandgap of LiBeN obtained in this work is in good agreement with previous calculations [37]. The band at Γ degenerates into flat and parabolic bands, and the flat band is along with $\Gamma - X$ and $\Gamma - L$ Directions. The degenerate flat band has a heavy effective mass, which is responsible for holes in the valence band. The heavy holes enhance this compound's thermoelectric performance and give a high rise value of the Seebeck coefficient. The parabolic band has an effective light mass that contributes to this compound's conductivity and is responsible for the high value of electrical conductivity. As reported in the literature, the combination of light holes and heavy holes yields high-performance thermoelectric properties. The band structure of LiMgN is given in Figure 1, and this band structure has the same features as the band structure of LiBeN. LiMgN has a direct bandgap of 2.37eV that occur at Γ point. The gap is given in Table 1 and is in excellent agreement with previous theoretical results compared with the available work in Table 1. As in the LiBeN band structure, the valence band at Γ point is degenerate into the flat band and parabolic band along $\Gamma - L$ and $\Gamma - X$ directions. The flat band in the case of LiMgN is flatter than that of LiBeN. The presence of these flat bands and parabolic implies high thermoelectric performance. The band structure of LiCaN is displayed in Figure 1. The maximum occupied state in the valence band occurs at X, and the minimum unoccupied state in the conduction band occurs at Γ points of LiCaN band structure, i.e. LiCaN is a direct bandgap compound. The value of the bandgap of LiCaN is 2.30eV and is in good agreement with the previous theoretical result as it is compared as shown in Figure 2. The valence band of LiCaN is degenerate into flat bands at Γ point; the flat band contains heavy holes and contributes to the Seebeck coefficient's high value. The band structure of LiSrN is given in Figure 1, it has an indirect bandgap between K and Γ point. The bandgap of LiSrN is 1.25eV and this value is in good agreement with previous work[**?**]. The band of LiSrN at Γ degenerates into flat bands, and these flat bands are parallel to the Fermi level. The parabolic bands are absent in the band structure of LiSrN. The band structure of LiBaN is displayed in Fig 1, and it has an indirect band of 1.01eV that occurs between X point and Γ point.

Table 1: Table of Structures, total energy and equilibrium lattice constants of LiYN(Y = Be, Mg, Ca, Sr and Ba)

Comps	Phases	Lat. constant	Etot
	α	4.39	-49.98995835
LiBeN	β	4.37	-50.23873147
	γ	4.33	-50.14184439
	α	4.86	-184.65282069
LiMgN	β	4.99	-184.80694627
	γ	5.05	-184.65378981
	α	5.26	-176.82092470
LiCaN	β	5.52	-176.92975996
	γ	5.57	-176.76451325
	α	5.60	-303.30515615
LiSrN	β	5.88	-303.59843891
	γ	5.92	-303.44347820
	α	5.98	-479.39819470
LiBaN	β	6.22	-479.48803298
	γ	6.23	-479.34924388

The valence band of LiBaN degenerates to flat bands without any parabolic band. Due to the GGA underestimation of the bandgap, the bandgaps obtained in this calculation are underestimated by 1.5±0.5eV. The bandgaps of LiYN(Y=Be, Mg, Ca, Sr, and Ba) decrease down the group of Y atoms and the largest bandgap with LiBeN and the smallest bandgap with LiBaN. The nature of the bandgap also changes from direct to indirect bandgap down the group. The degenerate bands change from a mixture of parabolic bands and flat bands to purely flat bands down the group.

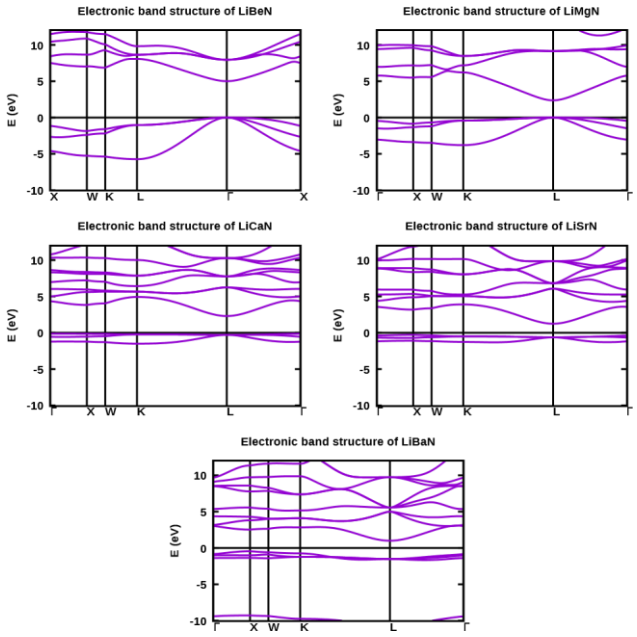

Figure 2: Band structure of LiYN (Y = Be, Mg, Ca, Sr and Ba)

Compounds	**a(Å)**	$E_g(eV)$
LiBeN	4.37[20] [37]	2.80[37]
LiMgN	4.99[33][38]	2.37[39]
LiCaN	5.52[21] [40]	2.30[40][20]
LiSrN	5.88[34]	1.25[34]
LiBaN	6.22	1.01

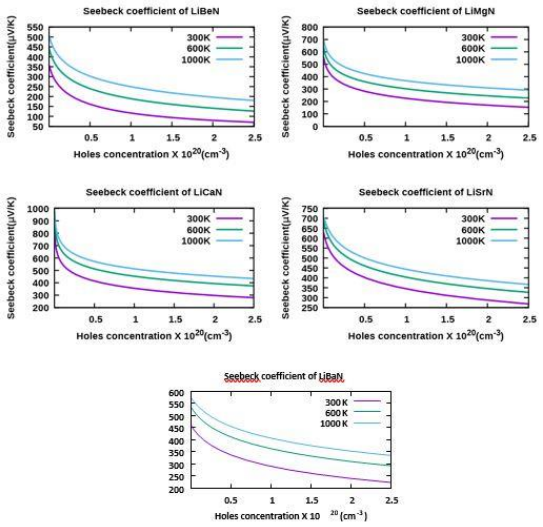

Figure 3: Seebeck coefficient of LiYN(Y = Be, Mg, Ca, Sr and Ba.)

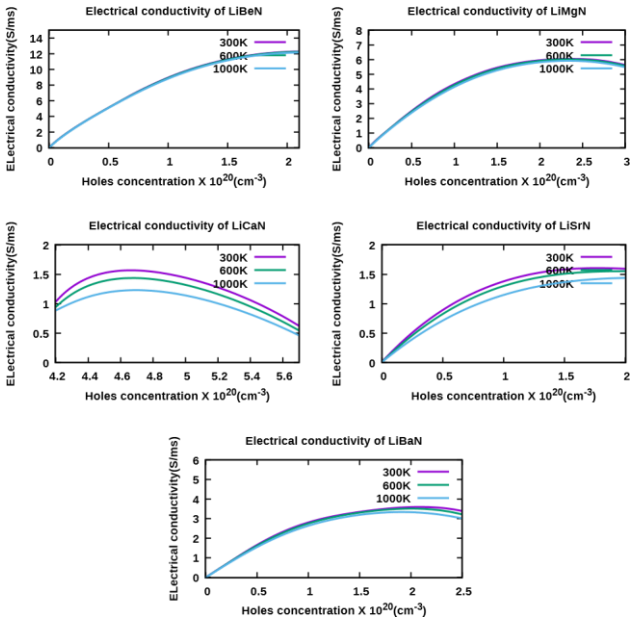

Figure 4: Electrical conductivity of LiYN(Y = Be, Mg, Ca, Sr and Ba.)

3.3 Thermoelectric Properties of LiYN(Be, Mg, Ca, Sr and Ba)

The performance of thermoelectric materials depends on the Seebeck coefficient(S), electrical conductivity(σ), thermal conductivity(k), power factor(PF), and dimensionless figure of merit(ZT). The values of S and σ depend on the combination of flat band and parabolic band, which has been observed to enhance thermoelectric performance materials[35]. The flat band enhances the Seebeck coefficient value while the parabolic band contributes to the value of electrical conductivity.

Figure 2 gives the Seebeck coefficient of these compounds. The HH compounds are at best performance around the temperature of 1000K. The Seebeck coefficient obtained in this work increases with an increase in temperature, as displayed in Figure 2. The values of Seebeck coefficients of LiYN(Y=Be, Mg, Ca, Sr, and Ba) at 1000K are 508.13μV/K for LiBeN, 700.01μV/K for LiMgN, 983.19μV/K for LiCaN, 706.47μV/K for LiSrN and 577.18μV/K for LiBaN. From the band structures in Figure 1, it's observed that the degenerate parabolic band in the LiBeN band structure starts to flatten. Pure flat band and flatten parabolic band are observed in the band structure of LiCaN; the mixture of these bands is responsible for the highest value of the Seebeck coefficient of LiCaN among these compounds.

Figure 3 gives electrical conductivity as a function of carrier concentration at 300K, 600K, and 1000K. The electrical conductivity of these compounds has an inversely proportional relationship with temperature. These compounds' electrical conductivity is maximum in the carrier concentration range of $1.95 - 4.67 \times 1020 cm^{-3}$. The maximum value of electrical conductivity of these compounds at 1000K are 3.34S/sm at $1.95 \times 1020 cm^{-3}$, 12.16S/sm at $2.14 \times 1020 cm^{-3}$, 5.93S/sm at $2.34 \times 1020 cm^{-3}$, 1.24S/sm at $4.67 \times 1020 cm^{-3}$ and 1.44S/sm at $2.00 \times 1020 cm^{-3}$ for LiBeN, LiMgN, LiCaN, LiSrN, and LiBaN respectively. The electrical conductivity of LiBeN is the highest among these compounds, and this is due to the parabolic degenerate valency band in the band structure of LiBeN. The parabolic bands have light-effective mass carriers, and the light-effective mass carriers enhance conductivity. The electrical conductivity of LiCaN is the least and is due almost to flatten band in the valence band. The flattened band is parallel to the Fermi level, and it has heavy effective mass carriers responsible for low conductivity.

Figure 4 gives these compounds' thermal conductivity follows the same trend as that of the electrical conductivity. Thermal conductivity obtained here increases with an increase in temperature. LiBeN has a thermal conductivity of 28.65W/msK, which is the highest thermal conductivity of LiYN(Y = Be, Mg, Ca, Sr and Ba), and the lowest value of thermal conductivity is that of LiCaN with the value of 2.16W/msK. The thermal conductivity of these compounds makes them potential candidates for microelectronics in which they can be used as heat absorbers.

Figure 5 gives the power factor of LiYN(Y = Be, Mg, Ca, Sr, and Ba.) as a function of carrier concentration. The maximum values of the power factor of these compounds are $12.28 W/msK^2$, $19.04 W/msK^2$, $11.86 W/msK^2$, $11.42 W/msK^2$ and $17.30 W/msK^2$ for LiBeN, LiMgN, LiCaN, LiSrN, and LiBaN respectively. The power factor of $19.04 W/msk^2$ for LiMgN is in good agreement with the value obtained in previous work [32]. The power factor obtained increases with temperature, and all the compounds have the highest power factor at 1000K. The power factor of LiMgN at 1000K is the highest in this work because LiMgN has a relatively high Seebeck coefficient and high electrical conductivity.

The dimensionless figure of merit of LiYN(Y = Be, Mg, Ca, Sr, and Ba) is displayed in Figure 6. The figure of merit measures the performance of materials such as

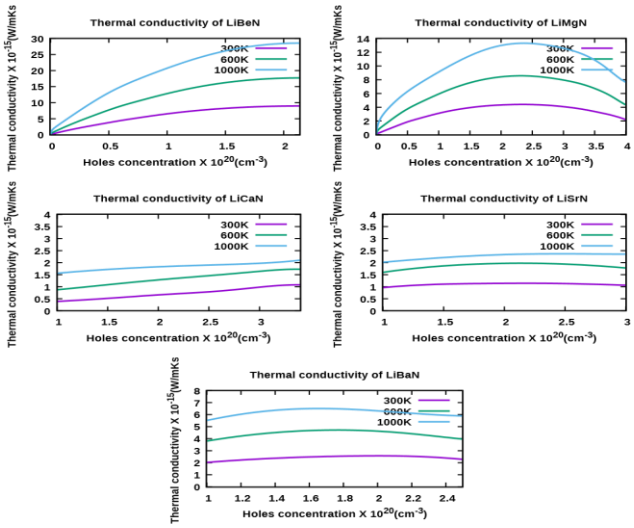

Figure 5: Thermal conductivity of LiYN(Y = Be, Mg, Ca, Sr and Ba.)

thermoelectric materials. The figure of merit of these compounds at 1000K as a function of carrier concentration are 0.94 at 5x1015cm^{-3} for LiBeN, 0.96 at 4x1016cm^{-3} for LiMgN, 0.99 at 1x1018cm^{-3} for LiCaN, 0.95 at 5x1017cm^{-3} for LiSrN and 0.95 at 6x1017cm^{-3} for LiBaN. The results of the figure of merits obtained in this work show that LiCaN has the highest value due to the perfect flat band and moderate parabolic band in the band structure of LiCaN. The highest value of the Seebeck coefficient of LiCaN results from a perfect flat band in the valence band.

The Electronic Fitness Function (EFF) of LiYN (Y = Be, Mg, Ca, Sr, and Ba) is displayed in Figure 7. EFF is an important parameter that is used to screen thermoelectric materials [36]. The inverse relationship between the Seebeck coefficient and electrical conductivity poses a difficulty. EFF annul the difficulty in optimization of electrical conductivity and Seebeck coefficient, therefore, it is necessary to calculate EFF of materials. The EFF of these compounds at $1000K$ are $1.3x10^{-19}W^{-5/3}ms^{-1/3}K^{-2}$, $1.0x10^{-19}W^{-5/3}ms^{-1/3}K^{-2}$, $0.\ 0.65x10^{-19}W^{-5/3}ms^{-1/3}K^{-2}$, and$1.1x10^{-19}W^{-5/3}ms^{-1/3}K$ respectively for LiBeN, LiMgN, LiCaN, LiSrN, and LiBaN.

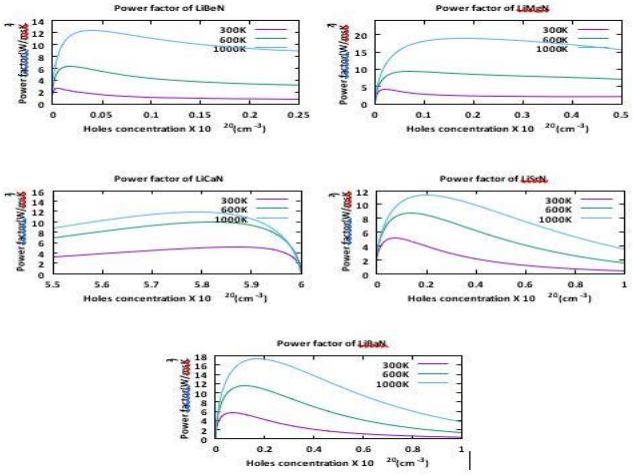

Figure 6: Power factor of LiYN(Y = Be, Mg, Ca, Sr and Ba.)

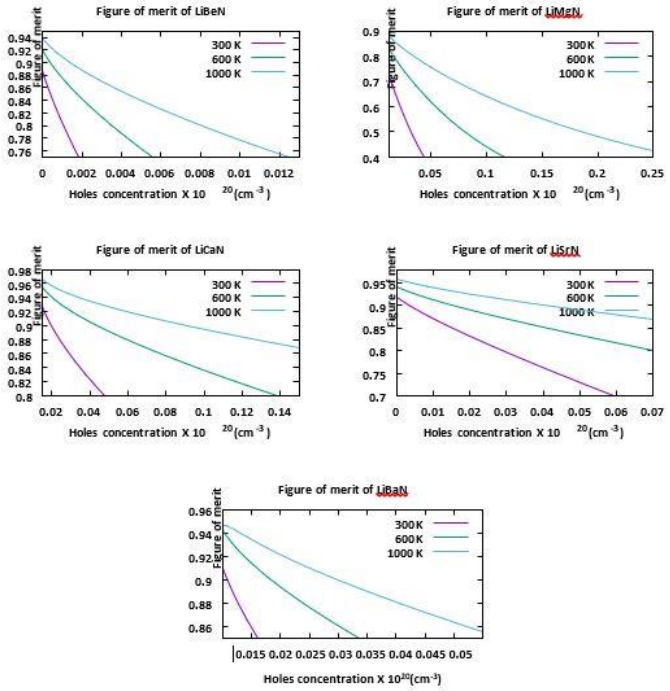

Figure 7: Figure of merit of LiYN(Y = Be, Mg, Ca, Sr and Ba.)

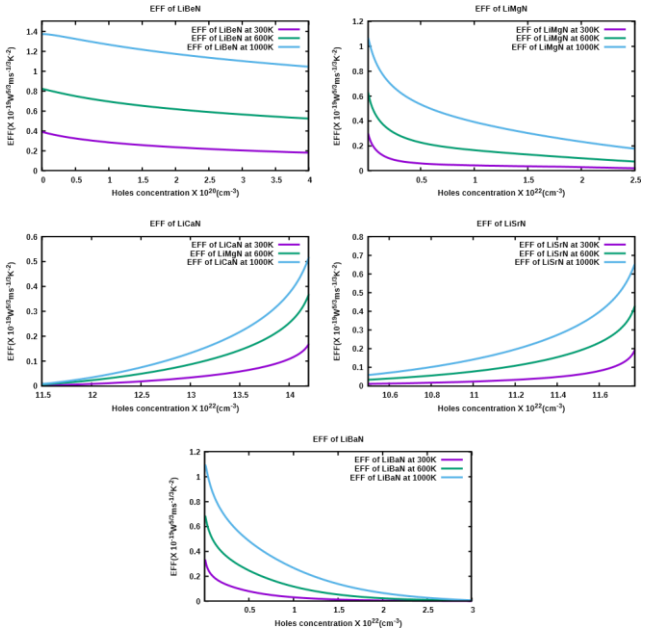

Figure 8: EFF of LiYN(Y = Be, Mg, Ca, Sr and Ba.)

4 CONCLUSION

The structural properties of LiYN (Y = Be, Mg, Ca, Sr, and Ba) have been calculated, and the most stable phase of these compounds is reported in this work. The band structures of these compounds have been critically examined in relation to thermoelectric properties. The transport coefficients like the Seebeck coefficient, electrical conductivity, electronic thermal conductivity, power factor, EFF, and merit figure have been calculated. From the results obtained in this work, all these compounds are candidates for high-performance thermoelectric material. LiCaN with the highest value of ZT will be the best thermoelectric candidate among these compounds.

AUTHORS' CONTRIBUTIONS

All authors participated actively in this research work and have read and approved the final manuscript.

CONSENT

All authors have approved the Consent form.

REFERENCES

1 Sztekler K, Wojciechowski K, Komorowski. The thermoelectric generators use for waste heat utilization from conventional power plant. Energy and Fuels. E3S Web of Conferences 2017;14(01032):1-8 DOI:10.1051/e3sconf/20171401032.

2 World Energy Resources. 2016; http://www.worldenergy.org/

3 Kardasz P, Wróbel R, Doskocz J, Wiejkut P. The energy harvesting from waste heat. World Scientific News. 2016;48(133):53-68.

4 Patowary R, and Baruah DC. International Journal of Energy Research. 2018;42(8), 2595-2614. https://doi.org/10.1002/er.4021

5 Zhan T, Yamato R, Hashimoto S, Tomita M, Oba S, Himeda Y et al. Miniaturized planar Si-nanowire micro-thermoelectric generator using exuded thermal field for power generation. Science and Technology of Advanced Materials. 2018 Dec 31;19(1):443453. doi: 10.1080/14686996.2018.1460177. Petsagkourakis Petsagkourakis I, Tybrandt K, Crispin X, Ohkubo I, Satoh N, Mori T. Thermoelectric materials and applications for energy harvesting power generation. Sci Technol Adv Mater. 2018;19(1):836-862. doi: 10.1080/14686996.2018.1530938.

6 Venkatasubramanian R, Siivola E, Colpitts T, O'Quinn B. Thin-film thermoelectric devices with high room-temperature figures of merit. Nature. 2001;413(6856):597-602. doi: 10.1038/35098012.

7 Heremans JP, Jovovic V, Toberer ES, Saramat A, Kurosaki K, Charoenphakdee A, Yamanaka S, Snyder GJ. Enhancement of thermoelectric efficiency in PbTe by distortion of the electronic density of states. Science. 2008 Jul 25;321(5888):554-7. doi: 10.1126/science.1159725. PMID: 18653890.

8 Gatti C, Bertini L, Blake NP, and Iversen BB. Chemistry. 2003;9(18): 4556–68. doi:10.1002/chem.200304837

9 Yin Y, Tudu B, and Tiwari A. Recent advances in oxide thermoelectric materials and modules. Vacuum 2017;146:356–374. doi:10.1016/j.vacuum.2017.04.015

10 Rogl G, and Rogl P. Skutterudites, a most promising group of thermoelectric materials. Current Opinion in Green and Sustainable Chemistry. 2017;4:50–57. doi:10.1016/j.cogsc.2017.02.006

11 Huang L, Zhang Q, Yuan B, Lai X, Yan X, and Ren Z. Recent progress in half-Heusler thermoelectric materials. Materials Research Bulletin 2016;76:107–112. doi:10.1016/j.materresbull.2015.11.032

12 He J, Naghavi S S, Hegde V I, Amsler M, and Wolverton C. Designing and Discovering a New Family of Semiconducting Quaternary Heusler Compounds Based on the 18-Electron Rule. Chemistry of Materials 2018;30(15), 4978–4985. doi:10.1021/acs.chemmater.8b01096 10.1021/acs.chemmater.8b01096

13 Grytsiv A, Romaka V V, Watson N, Rogl G, Michor H, Hinterleitner B, Rogl P. Thermoelectric Half-Heusler compounds TaFeSb and Ta1-xTixFeSb (0 ≤ x ≤ 0.11): Formation and physical properties. Intermetallics 2019; 111: 106468. doi:10.1016/j.intermet.2019.04.011.

14 Anand S, Xia K I, Hegde V, Aydemir U, Kocevski V, Zhu T, and Snyder G J. A valence balanced rule for the discovery of 18-electron half-Heuslers with defects. Energy and Environmental Science 2018;11(6): 1480–1488. doi:10.1039/c8ee00306h.

15 Poon S J. Half Heusler compounds: promising materials for mid-to-high temperature thermoelectric conversion. Journal of Physics D: Applied Physics 2019;52(49):493001. doi:10.1088/1361-6463/ab3d71

16 Fang T, Zhao, X, and Tiejun Zhu. ”Band Structures and Transport Properties of High-Performance Half-Heusler Thermoelectric Materials by First Principles.” Materials 2018;11(5): 847. https://doi.org/10.3390/ma11050847.

17 Mallick M M, Rajput K, and Vitta S. Increasing figureof-merit of ZrNiSn half-Heusler alloy by minimal substitution and thermal conductivity reduction. Journal of Materials Science: Materials in Electronics. 2019; doi:10.1007/s10854-019-00915-y

18 Vikram , Sahni B, Barman C K, and Alam A. Accelerated Discovery of New 8-Electron Half-Heusler Compounds as Promising Energy and Topological Quantum Materials. J. Phys. Chem. C 2019;123:7074−7080. doi:10.1021/acs.jpcc.9b01737

19 Bouhemadou A, Bin-Omran S, Allali D, Al-Otaibi S M, Khenata R, Al-Douri Y, Chegaar M, and Reshak A. H. Electronic and optical properties of the LiCdX (X = N, P, As and Sb) filled-tetrahedral compounds with the Tran–Blaha modified Becke–Johnson density functional. Materials Research Bulletin 2015;64:337-346. https://doi.org/10.1016/j.materresbull.2015.01.003.

20 Kacimi S, Mehnane H, and Zaoui A. I–II–V and I–III–IV half-Heusler compounds for optoelectronic applications: Comparative ab initio study. Journal of Alloys and Compounds 2014;587:451-458. https://doi.org/10.1016/j.jallcom.2013.10.046.

21 Kieven D, Klenk R, Naghavi S, Felser C, and Gruhn T. I-II-V half-Heusler compounds for optoelectronics: Ab initio calculations. Physical Review B, 2010;81(7). doi:10.1103/physrevb.81.075208.

22 Cherchab Y, and González-Hernández R. Structural stability and thermoelectric properties of new discovered half-Heusler KLaX (X = C, Si, Ge, and Sn) compounds. Computational and Theoretical Chemistry. 2021; 1200(113231):1-9. doi:10.1016/j.comptc.2021.113231

23 Reshak AH. Nowotny–Juza NaZnX (X = P, As, and Sb) as photovoltaic materials. Solar Energy. 2015;115: 430–440. doi:10.1016/j.solener.2015.03.01110.

24 Verma P, Singh C, Kamlesh P K. et al. NowotnyJuza phase KBeX (X=N, P, As, Sb, and Bi) halfHeusler compounds: applicability in photovoltaics and thermoelectric generators. J Mol Model 2023;29:23. https://doi.org/10.1007/s00894-022-05433-z

25 ”URL http://www.quantum-espresso.org”,

26 Giannozzi P, Baroni S, Bonini N, Calandra M, Car R, Cavazzoni C, Ceresoli D, Chiarotti GL, Cococcioni M, Dabo I, Dal Corso A, de Gironcoli S, Fabris S, Fratesi G, Gebauer R, Gerstmann U, Gougoussis C, Kokalj A, Lazzeri M, Martin-Samos L, Marzari N, Mauri F, Mazzarello R, Paolini S, Pasquarello A, Paulatto L, Sbraccia C, Scandolo S, Sclauzero G, Seitsonen AP, Smogunov A, Umari P, Wentzcovitch RM. QUANTUM ESPRESSO: a modular and open-source software

project for quantum simulations of materials. J Phys Condens Matter. 2009;21(39):395502. doi: 10.1088/0953-8984/21/39/395502.

27 Giannozzi P, Andreussi O, Brumme T, Bunau O, Buongiorno Nardelli M, Calandra M, Car R, Cavazzoni C, Ceresoli D, Cococcioni M, Colonna N, Carnimeo I, Dal Corso A, de Gironcoli S, Delugas P, DiStasio RA Jr, Ferretti A, Floris A, Fratesi G, Fugallo G, Gebauer R, Gerstmann U, Giustino F, Gorni T, Jia J, Kawamura M, Ko HY, Kokalj A, Küçükbenli E, Lazzeri M, Marsili M, Marzari N, Mauri F, Nguyen NL, Nguyen HV, Otero-dela-Roza A, Paulatto L, Poncé S, Rocca D, Sabatini R, Santra B, Schlipf M, Seitsonen AP, Smogunov A, Timrov I, Thonhauser T, Umari P, Vast N, Wu X, Baroni S. Advanced capabilities for materials modelling with Quantum ESPRESSO. J Phys Condens Matter. 2017 Nov 22;29(46):465901. doi: 10.1088/1361-648X/aa8f79.

28 Perdew JP, Burke K, Ernzerhof M. Generalized Gradient Approximation Made Simple. Phys Rev Lett. 1996;77(18):3865-3868. doi: 10.1103/PhysRevLett.77.3865.

29 Dal Corso A. Pseudopotentials periodic table: From H to Pu. Computational Materials Science 2014;95:337–350. doi:10.1016/j.commatsci.2014.07.043.

30 H. J. Monkhorst, J. D. Pack, Phys. Rev. B 13 (1976) 5189

31 Madsen GK, and Singh DJ. BoltzTraP. A code for calculating band-structure dependent quantities.

Computer Physics Communications 2006;175(1):67-71. https://doi.org/10.1016/j.cpc.2006.03.007

32 Ahmed, R. and Masuri, N. S. and Ul Haq, B. and Shaari, A. and AlFaifi, S. and Butt, F. K. and Muhamad, M. N. and Ahmed, M. and Tahir, S. A. (2017) Investigations of electronic and thermoelectric properties of half-Heusler alloys XMgN (X = Li, Na, K) by first-principles calculations. Materials and Design 2017;136:196-203.

33 Yadav MK, and Sanyal B. First-principles study of thermoelectric properties of Li-based half-Heusler alloys. Journal of Alloys and Compounds 2015;622:388-393.
https://doi.org/10.1016/j.jallcom.2014.10.025

34 Benazouzi Y, Rozale H, Boukli Hacene MA, Khethir M, Chahed A, and Lucache D. Electronic and Thermoelectric Properties in Li-Based Half-Heusler Compounds: A First Principle Study. Annals of West University of Timisoara - Physics 2019;61(1):44–55. doi:10.2478/awutp-2019-0004

35 Yang G, Yang J, Yan Y, Wang Y. The relationship between the electronic structure and thermoelectric properties of Zintl compounds M2Zn5As4 (M = K, Rb). Physical Chemistry Chemical Physics 2014;16(12):5661.
doi:10.1039/c3cp54545h

36 Xing G, Sun J, Li Y, Fan X, Zheng W, and Singh DJ.
Electronic fitness function for screening semiconductors as thermoelectric materials. Physical Review Materials 2017;1(6). doi:10.1103/physrevmaterials.1.065405.

37 Yu L, Yao K, Liu Z, and Zhang Y. Electronic structure of half-Heusler semiconductor LiBeN. Physics Letters A 2007;367(4-5):389-393.
https://doi.org/10.1016/j.physleta.2007.03.092

38 Anuradha, Kaur K, Singh R, and Kumar R. Materials Research Express 2018;5(1):014009.

39 Arif M, Murtaza G, Ali R, Khenata R, Takagiwa Y, Muzammil M, and Omran SB. Elastic and electro-optical properties of XYZ (X = Li, Na and K; Y = Mg; Z = N, P, As, Sb and Bi) compounds. Indian Journal of Physics 2015;90(6):639–647. doi:10.1007/s12648-015-0791-8

40 Mehnane H, Bekkouche B, Kacimi S, Hallouche A, Djermouni M, and Zaoui A. First-principles study of new half Heusler for optoelectronic applications. Superlattices and Microstructures 2012;51(6):772-784. https://doi.org/10.1016/j.spmi.2012.03.020.